

Using Artificial Neural Networks for Estimation of Thermal Conductivity of Binary Gaseous Mixtures

Reza Eslamloueyan* and Mohammad Hasan Khademi

Chemical, Oil and Gas Engineering Department, Shiraz University, Zand Avenue, Shiraz, Iran

Prediction of gas thermal conductivity is crucial in the heat transfer process. In this article, we develop a novel method to estimate conductivities of binary gaseous mixtures at atmospheric pressure. The method is a neural network scheme consisting of two consecutive multilayer perceptrons (MLPs). The first MLP estimates pure component conductivities as a function of critical temperature, critical pressure, molecular weight, and temperature. The conductivities calculated in the first MLP as well as molecular weights of both compounds and mole fraction of the light components are fed to the second MLP to predict the thermal conductivity of the mixture. The proposed model was trained and tested through a large set of experimental data over wide ranges of temperatures, compositions, and substances. Comparing the test and training results indicates that the accuracy of the neural model is remarkably better than other alternative methods proposed in the literature. Conventional conductivity correlations require more input parameters which are not available for many gases. Also, correlations recommended for pure gas conductivity are usually valid for a particular range of temperature and substances. However, the MLP scheme is able to cover a wide range of temperatures and substances with a few numbers of parameters which are abundant for most gases.

Introduction

Thermal conductivity of gases is one of the most important thermal properties since it is needed in the analysis of heat transfer equipment. Data on thermal conductivity are required for mathematical modeling and computer simulation of heat transfer processes. Over the years, the thermal conductivity has been measured and compiled for many gases. Generally, the estimation methods of thermal conductivity of pure gases can be classified into two wide categories. In one category, thermal conductivity is estimated through using relations based on the theory of gases. For example, Pidduck extended the Chapman–Enskog method of an infinitely dilute gas of spherical molecules to the case of rigid spherical molecules having rotational energy convertible to translational energy.¹ Eucken² investigated the influence of internal degree of freedom on conductivity of a dilute gas of a polyatomic molecule and proposed a correlation based on the ratio of heat capacities at constant pressure and constant volume. Ubbelohde assumed that the molecules of a dilute gas at different energy states could be considered as chemical species, and the flux of energy was connected to the diffusion of these species.³ The first work on calculation of dense gas conductivity based on the hard sphere model was done by Enskog.⁴ Longuet-Higgins and Pople developed a correlation for conductivity of a dense gas assuming the existence of a collision mechanism.⁵ Some other studies in this category are given in the references.^{6–13}

The second category consists of correlations relating thermal conductivity to other measurable properties such as critical temperature, critical pressure, and molecular weight. For instance, Misic and Thodos developed two different correlations for thermal conductivity of low-pressure pure hydrocarbon gases.^{14,15} One of their correlations was suggested for methane

and cyclic compounds below reduced temperatures of 1.0, and the other correlation was recommended for higher reduced temperatures as well as the rest of the hydrocarbons at any temperature. Bromley and Wilke suggested correlations for pure nonhydrocarbon monatomic and linear molecules at low pressure (less than 1 atm).^{16,17} Pliński estimated the thermal conductivity of CO₂, N₂, He, Xe, CO, O₂, and Ar as a function of temperature.¹⁸ Also, Stiel and Thodos proposed an equation to predict the thermal conductivity of nonlinear molecules of nonhydrocarbon gases at low pressure.¹⁹

Heating or cooling of gaseous mixtures has many applications in process industries. Estimation of thermal conductivity of a gaseous mixture plays an important role in the design of heat exchangers involving gaseous mixtures. The determination of the thermal conductivity of gaseous mixtures is more complex than pure gases, from both the theoretical and experimental points of view. The thermal conductivity of a gas mixture cannot be simply predicted through linear combination of conductivities of the individual component gases. A number of methods have been developed for estimating the thermal conductivity of gaseous mixtures. The choice of a particular method depends mainly upon available parameters and the desired accuracy of estimation. Muckenfuss and Curtiss²⁰ proposed a formula for the thermal conductivity of an *n*-component gas mixture. Mason and Saxena showed that the formula of Muckenfuss and Curtiss has two disadvantages from a practical viewpoint.²¹ First, the formula is quite complicated and involves laborious computation. Second, it requires a reliable knowledge of force laws for the various molecular interactions, which are rarely available. To overcome these difficulties, Mason and Saxena²¹ suggested the following approximate formula

$$\lambda_{\text{mix}} = \sum_{i=1}^n \lambda_i \left[1 + \sum_{\substack{k=1, \\ k \neq i}}^n G_{ik} \frac{x_k}{x_i} \right]^{-1} \quad (1)$$

where

* Corresponding author. Fax: 98-711-6287294. E-mail: eslamlo@shirazu.ac.ir.

$$G_{ik} = \frac{1.065}{2\sqrt{2}} \left(1 + \frac{M_i}{M_k}\right)^{-\frac{1}{2}} \left[1 + \left(\frac{\lambda_i^0}{\lambda_k^0}\right)^{\frac{1}{2}} \left(\frac{M_i}{M_k}\right)^{\frac{1}{4}}\right]^2 \quad (2)$$

where M is molecular weight; x is component mole fraction in the mixture; λ is thermal conductivity of the pure component; and λ_{mix} is gas mixture thermal conductivity. G_{ki} is obtained from G_{ik} by interchanging the subscripts, and λ_i^0 is the frozen thermal conductivity of a pure gas from the following relation

$$\lambda_i^0 = \lambda_i [0.115 + 0.354\gamma/(\gamma - 1)]^{-1} \quad (3)$$

where γ is the ratio of specific heat of a gas at constant pressure to that at constant volume. Lindsay and Bromley²² suggested that G_{ik} in eq 1 be determined from the relation

$$G_{ik} = \frac{1}{4} \left[1 + \left\{\frac{\eta_i \left(\frac{M_k}{M_i}\right)^{3/4} (1 + S_i/T)}{\eta_k \left(\frac{M_i}{M_k}\right)^{3/4} (1 + S_k/T)}\right\}^{1/2}\right]^2 \frac{1 + S_{ik}/T}{1 + S_k/T} \quad (4)$$

where η_i and S_i are the viscosity and Sutherland constant of a component, respectively. S_{ik} is the geometric mean of S_i and S_k . The Sutherland constant for all pure gases (with the exception of hydrogen, deuterium, and helium) was taken from the expression $S = 1.5T_b$, where T_b is the absolute boiling temperature at atmospheric pressure. For hydrogen, deuterium, and helium, the Sutherland constant was assumed to be equal to 79. It was shown that Lindsay and Bromley correlation does not yield accurate values for gas mixture thermal conductivity.^{23,24} Srivastava and Saxena modified eq 1 through introducing an additional unknown constant being determined from the value of mixture conductivity (λ_{mix}) at a given composition.²³ Ulybin et al.²⁵ used an empirical procedure for computing the thermal conductivity of a binary mixture at a higher temperature from the known thermal conductivity of the mixture at some lower temperature

$$\lambda_{\text{mix}}(T_2) = \lambda_{\text{mix}}(T_1) \left[x_1 \frac{\lambda_1(T_2)}{\lambda_1(T_1)} + x_2 \frac{\lambda_2(T_2)}{\lambda_2(T_1)} \right] \quad (5)$$

Hirschfelder²⁶ derived the expression for the thermal conductivity of a binary mixture involving polyatomic gases

$$\lambda_{\text{mix}} = \lambda_{\text{mix}}^0 + \frac{\lambda_1 - \lambda_1^0}{1 + \frac{D_{11}x_2}{D_{12}x_1}} + \frac{\lambda_2 - \lambda_2^0}{1 + \frac{D_{22}x_1}{D_{12}x_2}} \quad (6)$$

$$\lambda_{\text{mix}}^0 = \frac{4(x_1^2 L_{22} - 2x_1x_2 L_{12} + x_2^2 L_{11})}{(L_{12}^2 - L_{11}L_{22})} \quad (7)$$

$$L_{11} = -\frac{4x_1^2}{\lambda_1^0} - \frac{16Tx_1x_2}{25PD_{12}(M_1 + M_2)^2} [(15/2)M_1^2 + (25/4)M_2^2 - 3M_2^2B_{12}^* + 4M_1M_2A_{12}^*] \quad (8)$$

$$L_{12} = \frac{16Tx_1x_2M_1M_2}{25PD_{12}(M_1 + M_2)^2} [(55/4) - 3B_{12}^* - 4A_{12}^*] \quad (9)$$

L_{22} is obtained from L_{11} by interchanging the subscripts. Here P is the pressure; D_{12} is the accurate value of the binary diffusion coefficient for components 1 and 2; D_{11} and D_{22} are self-diffusion coefficients for gases 1 and 2, respectively; and A_{12}^* and B_{12}^* are dimensionless ratios of certain collision integrals characterizing molecules of gases 1 and 2. The A_{12}^* and B_{12}^* are weakly affected by temperature change and the forces between molecules 1 and 2, so they are usually considered to be unity.

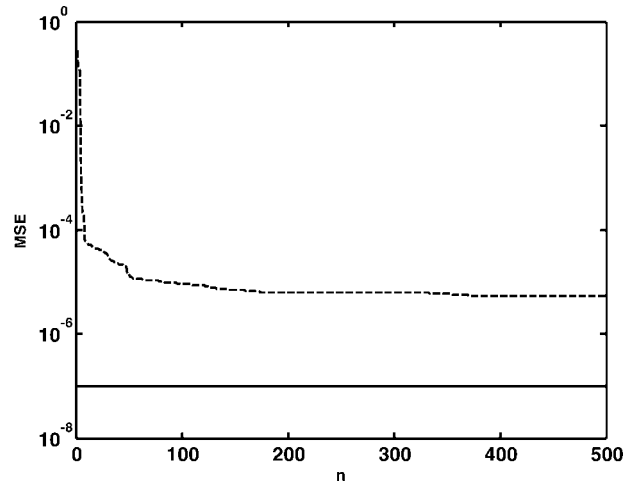


Figure 1. MSE versus iteration number (n) for MLP predicting pure gas conductivity. Solid line: goal; dashed line, training.

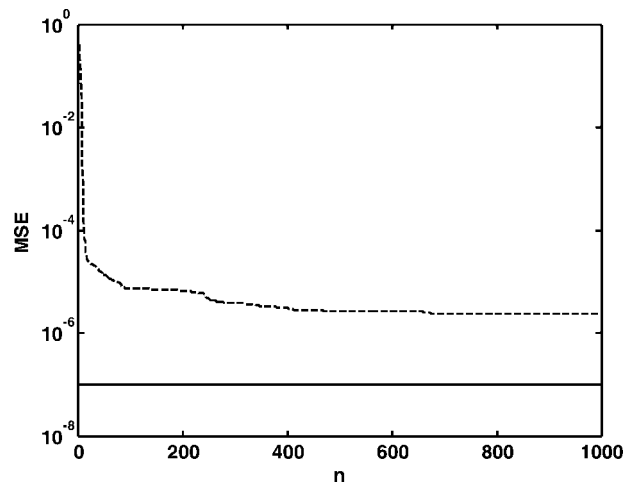


Figure 2. MSE versus iteration number (n) for MLP predicting conductivity of a binary gaseous mixture. Solid line, goal; dash line, training.

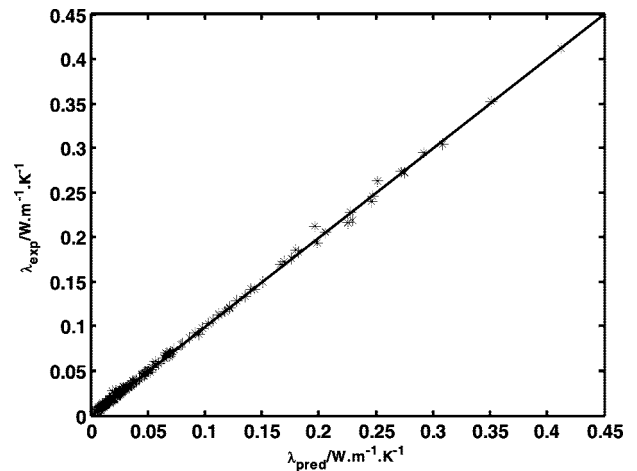


Figure 3. Correlation of training experimental data versus the predicted conductivities of the pure gases.

Neural networks have been used extensively in various fields of chemical engineering over the last two decades. Turias et al. studied the application of pattern recognition and artificial intelligence techniques in the characterization of a multiphase realistic disordered composite and in the design of a multiple regression model to estimate effective thermal conductivity.²⁷ Sablani and Rahman presented an artificial neural network

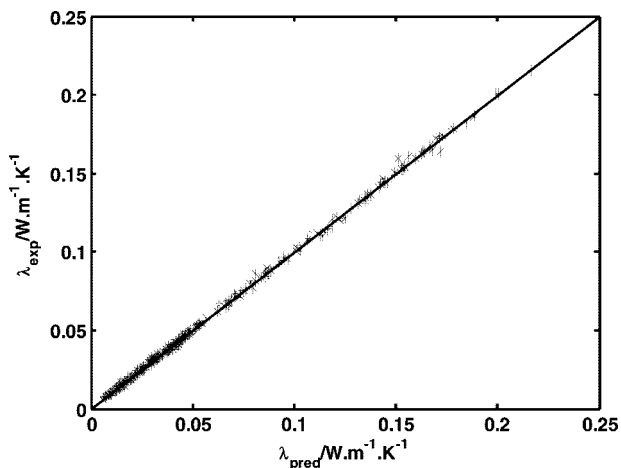


Figure 4. Correlation of training experimental data versus the predicted conductivities of the gaseous mixtures.

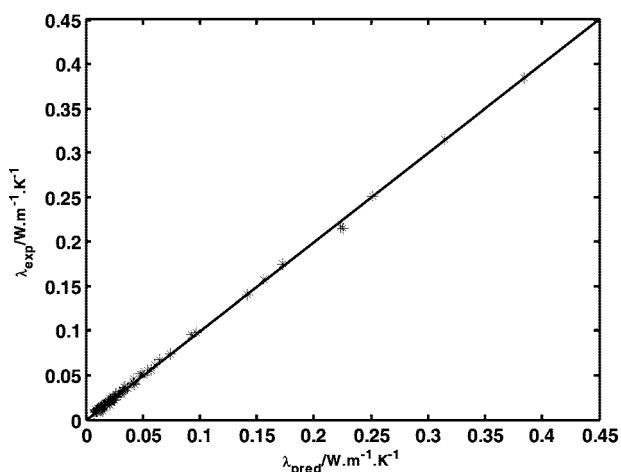


Figure 5. Correlation of the test experimental data versus the predicted conductivities of the pure gases.

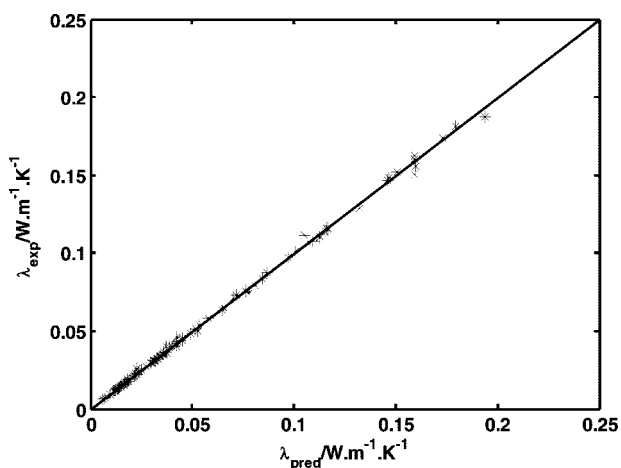


Figure 6. Correlation of the test experimental data versus the predicted conductivities of the gaseous mixtures.

model for the prediction of the thermal conductivity of food at different temperatures, moisture contents, and apparent porosities.²⁸ The model was able to predict thermal conductivity with a mean relative error of 12.6 %. Sablani et al. used artificial neural networks to estimate thermal conductivity of bakery.²⁹ Their model was able to predict thermal conductivity with a mean relative error of 10 %. Zhou et al. focused on modeling the electrical conductivity of recombined milk by artificial neural

Table 1. Range of Pure Gas Data Used in the Development of the ANN Model

no.	component type	no. of data points	T_i/K^a	P_i/bar^a	M^a
1	acetone	6	508.1	46.4	58.08
2	acetylene	9	308.3	61.4	26.038
3	ammonia	11	405.6	112.8	17.031
4	argon	10	150.8	48.7	39.948
5	benzene	8	562.05	48.95	78.114
6	bromine	3	584.1	103.0	159.808
7	carbon dioxide	22	304.2	73.8	44.01
8	carbon disulfide	2	552.0	78.0	76.131
9	carbon tetrachloride	5	556.4	45.0	153.823
10	chlorine	5	417.0	76.0	70.906
11	chloroform	3	536.4	54.0	119.378
12	cyclohexane	1	553.5	40.73	84.161
13	deuterium	3	38.4	16.4	4.032
14	ethane	6	305.32	48.72	30.07
15	ethyl acetate	3	523.2	38.3	88.11
16	ethyl chloride	4	460.4	52.0	64.515
17	helium	15	5.2	2.27	4.003
18	heptane	5	540.2	27.4	100.204
19	hexene	2	504.0	31.43	84.161
20	hydrogen	15	33.2	13.0	2.016
21	krypton	3	209.4	55.0	83.8
22	methane	8	190.6	46.0	16.043
23	methyl alcohol	2	512.64	80.97	30.042
24	methylene chloride	4	378.0	61.5	84.9
25	<i>n</i> -butane	4	425.12	37.96	58.123
26	neon	5	44.4	27.6	20.183
27	nitric oxide	3	180.0	65.0	30.006
28	nitrogen	14	126.2	33.9	28.013
29	nitrous oxide	2	309.6	72.4	44.013
30	<i>n</i> -pentane	4	469.7	33.7	72.15
31	oxygen	12	154.6	50.5	31.999
32	propylene	5	364.9	46.0	42.081
33	R 11 (trichlorofluoromethane)	2	471.1	44.72	137.368
34	R 12 (dichlorodifluoromethane)	6	385.1	41.3	120.913
35	R 13 (chlorotrifluoromethane)	4	302.0	38.7	104.459
36	R 22 (chlorodifluoromethane)	4	369.28	49.86	86.468
37	sulfur dioxide	5	430.8	77.8	64.063
38	water vapor	8	647.3	220.5	18.015
39	xenon	3	289.7	58.4	131.3

Total 236

^a Extracted from ref 38.

networks.³⁰ Jalali-Heravi et al. developed a neural network to predict the response factor of a thermal conductivity detector.³¹ Eslamloueyan and Khademi designed a multilayer perceptron for estimation of pure gas thermal conductivity.³² They used a set of 236 experimental data points for hydrocarbon and nonhydrocarbon compounds to develop their neuromorphic model. They showed that the proposed neural network outperforms other alternative methods, with respect to accuracy as well as extrapolation capabilities.

The objective of this work is to formulate a neural network scheme for prediction of thermal conductivities of binary gaseous mixtures at atmospheric pressure over a wide range of temperatures and compositions. The proposed scheme consists of two consecutive neural networks: the first one is used for pure gas conductivity and the second one for gaseous mixture conductivity.

Method

Artificial neural networks have the inherent characteristic of learning and recognizing nonlinear complex relationships, so they can be used to predict thermal conductivity of gas. The proposed method is based on multilayer perceptron (MLP) networks.

Table 2. Binary Gaseous Mixture Data Used for the Development of the ANN Model

no.	gas mixture	T	no. of data points	λ_2	λ_1	no.	gas mixture	T	no. of data points	λ_2	λ_1		
		K		$W \cdot m^{-1} \cdot K^{-1a}$	$W \cdot m^{-1} \cdot K^{-1a}$			K		$W \cdot m^{-1} \cdot K^{-1a}$	$W \cdot m^{-1} \cdot K^{-1a}$		
1	CH ₄ + nC ₄ H ₁₀	277.4	1	0.0328	0.0139	18	SO ₂ + Kr	394.46	3	0.0240	0.0126		
		310.7	1	0.0377	0.0165			434.26	3	0.0258	0.0143		
		344.1	1	0.0427	0.0193			473.76	3	0.0274	0.0161		
		377.4	1	0.0480	0.0224			312.16	3	0.0098	0.0104		
		410.7	1	0.0535	0.0257			353.26	3	0.0111	0.0122		
2	H ₂ + CO ₂	444.1	1	0.0593	0.0293	19	He + Xe	394.46	3	0.0126	0.0136		
		273.16	7	0.1696	0.0148			434.26	3	0.0143	0.0146		
		298.16	4	0.1820	0.0168			473.76	3	0.0161	0.0152		
		273.16	5	0.1696	0.0222			302.16	4	0.1499	0.0072		
		273.16	4	0.1696	0.0231			302.16	4	0.0100	0.0072		
3	H ₂ + CO	313.16	3	0.1892	0.0261	20	Kr + Xe	313.16	3	0.1892	0.0482		
		338.16	3	0.2008	0.0280			21	H ₂ + Ne	338.16	3	0.2008	0.0508
		368.16	3	0.2144	0.0302					366.16	2	0.2135	0.0541
4	H ₂ + N ₂	408.16	3	0.2325	0.0331	22	Ne + N ₂	368.16	1	0.2144	0.0544		
		448.16	3	0.2505	0.0359			408.16	2	0.2325	0.0597		
		273.16	5	0.1696	0.0147			448.16	2	0.2505	0.0652		
5	H ₂ + N ₂ O	295	4	0.1805	0.0262	23	D ₂ + N ₂	313.16	3	0.0482	0.0261		
		313.16	3	0.1892	0.0276			24	N ₂ + O ₂	338.16	2	0.0541	0.0300
		338.16	2	0.2008	0.0295					366.16	2	0.0544	0.0302
6	H ₂ + O ₂	366.16	3	0.2135	0.0316	25	H ₂ + Kr	368.16	1	0.0544	0.0302		
		273.16	3	0.0231	0.0173			408.16	2	0.0597	0.0331		
		273.16	3	0.1401	0.0173			448.16	2	0.0652	0.0359		
7	N ₂ + Ar	298.16	5	0.1820	0.0228	26	H ₂ + Xe	313.16	2	0.1471	0.0261		
		273.16	3	0.1401	0.0173			27	D ₂ + Xe	366.16	2	0.1650	0.0300
		298.16	5	0.1820	0.0228					368.16	2	0.1786	0.0331
8	He + Ar	273.16	3	0.1401	0.0173	28	Ar + Xe	448.16	2	0.1918	0.0359		
		298.16	5	0.1820	0.0228			29	H ₂ + Kr	313.16	3	0.1892	0.0375
		273.16	4	0.1696	0.1315					338.16	3	0.2008	0.0416
9	H ₂ + C ₂ H ₄	313.16	3	0.1892	0.1471	30	H ₂ + Kr	366.16	3	0.2135	0.0127		
		338.16	2	0.2008	0.1558			31	H ₂ + Xe	313.16	2	0.1892	0.0076
		366.16	3	0.2135	0.1650					338.16	3	0.2008	0.0085
10	H ₂ + D ₂	408.16	4	0.2325	0.1786	32	D ₂ + Xe	366.16	3	0.2135	0.0094		
		448.16	3	0.2505	0.1918			33	Ar + Xe	313.16	3	0.1471	0.0076
		298.16	3	0.0240	0.0228					338.16	3	0.1558	0.0085
11	NH ₃ + C ₂ H ₄	295.16	4	0.0237	0.0239	34	Ar + Xe	366.16	2	0.1650	0.0094		
		303.16	6	0.1503	0.0268			35	H ₂ + Kr	366.16	2	0.1650	0.0094
		318.16	8	0.1555	0.0280					366.16	2	0.1650	0.0094
12	NH ₃ + CO	303.16	6	0.1503	0.0268	36	H ₂ + Kr	313.16	3	0.1892	0.0105		
		318.16	8	0.1555	0.0280			37	H ₂ + Kr	338.16	3	0.2008	0.0116
		318.16	5	0.0473	0.0268					366.16	3	0.2135	0.0127
13	He + O ₂	313.16	2	0.0482	0.0276	38	H ₂ + Kr	366.16	3	0.2135	0.0127		
		318.16	6	0.0487	0.0280			39	H ₂ + Xe	313.16	2	0.1892	0.0076
		338.16	3	0.0508	0.0295					338.16	3	0.2008	0.0085
14	Ne + O ₂	368.16	3	0.0544	0.0318	40	D ₂ + Xe	366.16	3	0.2135	0.0094		
		408.16	3	0.0597	0.0347			41	D ₂ + Xe	313.16	3	0.1471	0.0076
		448.16	3	0.0652	0.0375					338.16	3	0.1558	0.0085
15	O ₂ + Kr	303.16	6	0.0268	0.0100	42	Ar + Xe	366.16	2	0.1650	0.0094		
		318.16	6	0.0280	0.0107			43	Ar + Xe	366.16	2	0.1650	0.0094
		318.16	6	0.0280	0.0107					366.16	2	0.1650	0.0094
16	O ₂ + Xe	303.16	6	0.0268	0.0072	44	Ar + Xe	313.16	2	0.0197	0.0076		
		318.16	6	0.0280	0.0078			45	Ar + Xe	338.16	2	0.0211	0.0085
		318.16	6	0.0280	0.0078					338.16	2	0.0211	0.0085
17	Ar + SO ₂	312.16	3	0.0197	0.0098	46	Ar + Xe	366.16	2	0.0226	0.0094		
		353.26	3	0.0220	0.0111			47	Ar + Xe	366.16	2	0.0226	0.0094
										Total		277	

^a Predicted by the first ANN at the desired temperature.**Table 3. Ranges of Data of Pure Component Properties**

property	minimum	maximum
T/K	90.2	2000
T_c/K	5.20	647.3
P_c/bar	2.27	220.5
M	2.016	159.808
$\lambda/W \cdot m^{-1} \cdot K^{-1}$	0.0038	0.412

Table 4. Ranges of Data of Binary Mixture Properties

property	minimum	maximum
$\lambda_2/W \cdot m^{-1} \cdot K^{-1}$	0.0098	0.2505
$\lambda_1/W \cdot m^{-1} \cdot K^{-1}$	0.0072	0.1918
M_2	2.016	83.8
M_1	4.032	131.3
x_2	0.0336	0.964
$\lambda_{\text{mix}}/W \cdot m^{-1} \cdot K^{-1}$	0.0061	0.2165

Artificial Neural Networks. Artificial neural networks (ANN) can be considered as a simplified mathematical formulation of the central neural system in human beings. They are implemented through computer programs or electronic hardware devices. In fact, ANNs mimic the computational abilities of biological neural systems by using numbers of simple intercon-

Table 5. MRE, MSE, and R Values for Different Neural Network Configurations

ANN	no. of neurons	MRE	MSE	R -value
first ANN	5	9.5	$1.2 \cdot 10^{-5}$	0.9986
	8	7.4	$7.5 \cdot 10^{-6}$	0.9991
	10	5.4	$3.8 \cdot 10^{-6}$	0.9996
	12	5.8	$3.9 \cdot 10^{-6}$	0.9996
	15	7.3	$6.4 \cdot 10^{-6}$	0.9993
second ANN	20	8.7	$1.4 \cdot 10^{-5}$	0.9983
	5	3.4	$5.6 \cdot 10^{-6}$	0.9989
	8	3.4	$5.5 \cdot 10^{-6}$	0.9989
	10	2.6	$5.8 \cdot 10^{-6}$	0.9988
	12	2.2	$3.3 \cdot 10^{-6}$	0.9993
	15	2.3	$3.8 \cdot 10^{-6}$	0.9992
	20	2.5	$5.7 \cdot 10^{-6}$	0.9988

nected so-called artificial neurons.³³ These artificial neurons are computational units which are connected together by means of direct communication links. The links multiply the received information from neurons by so-called weights and transfer the weighted information to other neurons in a predefined structure. The output of a neuron is computed from the following equation

$$O_j = f \left(\sum_{i=1}^n w_{ji} y_i + b_j \right) \quad (10)$$

where O_j = output of j th neuron; f = activation or transfer function; b_j = bias of j th neuron; w_{ji} = synaptic weight corresponding to i th synapse of j th neuron; y_i = i th input signal to j th neuron; n = number of input signals to j th neuron. As eq 10 shows, bias is an activation threshold added to the weighted average of neuron input. Different types of transfer functions have been used in ANNs: logarithmic sigmoid, hyperbolic tangent sigmoid, and linear functions. The weighted sum of all inputs plus the bias of the neuron become the input of the activation function. The activation function serves mainly as a type of filter that determines the strength of the neuron output. Differentiability is an important characteristic of an activation function since it facilitates the network training. Some types of ANNs have been developed and used for different applications: multilayer perceptron (MLP), radial basis function (RBF), ART, and auto associative networks.³⁴ MLP networks are the most commonly used ones for the function approximation. MLP networks consist of groups of interconnected neurons arranged in layers corresponding to input, hidden, and output layers.

The input layer receives all input signals and dispatches them to other neurons. The network's outputs which are provided by the neurons in the output layer are actually the final results of the neuromorphic model. Consequently, the number of neurons for the input and output layers is defined by the number of independent and dependent variables, respectively. The input layer is fed with input variables and passes them into the hidden layer(s) where the processing task takes place. Finally, the output layer receives the information from the last hidden layer and sends the results to an external source. The network resembles an input/output model, whose parameters are synaptic weights and biases. This type of network has the potential of approximating most types of nonlinear functions, irrespective of how complex they are.³⁴

Table 6. Parameters (Weight and Bias) of the First ANN

neuron	hidden layer				biases	output layer	
	weights					weights	bias
	T	T_c	P_c	M			
1	0.0056	0.0087	-0.0851	0.5484	-1.9631	0.0266	0.2593
2	0.0014	0.0001	-0.0037	-0.0029	-2.2370	1.6606	
3	0.0025	0.0125	-0.0317	-0.2144	0.1724	0.0832	
4	0.0014	-0.0025	0.0027	0.0012	-2.1738	-1.6061	
5	-0.0077	-0.0468	0.1674	-0.1409	2.1109	0.0272	
6	-0.0007	0.0070	-0.0016	-0.0000	-1.3710	-0.0809	
7	0.0007	0.0041	0.0020	0.0002	-2.1501	-0.7887	
8	0.0006	0.0036	0.0020	0.0004	-1.8533	0.9033	
9	-0.0019	-0.8016	1.8916	0.5834	2.6549	-0.1497	
10	0.0013	-0.0311	0.0659	-0.0306	0.1766	0.2493	

Table 7. Parameters (Weight and Bias) of the Second ANN

neuron	hidden layer					output layer		
	weights					biases	weights	
	λ_2	λ_1	M_2	M_1	x_2		λ_{mix}	bias
1	-24.027	-9.1178	0.2160	1.1079	-0.2562	2.5745	5.9372	0.0290
2	-6.8484	3.8835	-2.4926	0.9023	9.4038	-20.517	-0.0046	
3	23.4736	9.6501	0.2502	-0.1586	0.2556	-7.3071	5.9880	
4	1.6359	-8.0949	0.0020	-0.0000	-0.0412	-1.5214	-0.9945	
5	8.6869	19.165	-0.1552	0.2854	0.1467	-2.3386	-1.7814	
6	-2.3418	4.5377	0.0316	0.0000	-1.0985	2.1296	-0.5704	
7	-9.7146	4.7798	-0.7689	0.0727	4.3115	0.8415	0.0117	
8	-1.8480	20.783	0.4488	0.0029	7.4425	-5.9777	-0.0046	
9	7.6187	-2.2780	-3.5288	3.3652	-12.264	0.4530	0.0049	
10	-8.0066	-4.8437	-0.1403	0.0020	0.5253	0.7829	-0.0658	
11	-4.3437	1.8629	0.0067	-0.0105	0.1457	-1.9038	-1.4435	
12	-14.843	-9.8215	-1.3295	0.7795	5.1496	-2.1681	-0.0074	

During the training algorithm, input data are fed to the input layer of the network. The difference between the output layer results, and the desired outputs (i.e., network error) is used as a criterion for adjustment of the network's synaptic weights and biases. At the beginning, all synaptic weights and biases are initialized randomly. Then, the network is trained based on an error index and an optimization algorithm until it correctly simulates the input/output mapping.

The required number of training data points and hidden layer neurons are the two challenges that have to be tackled appropriately. Some heuristics guidelines suggest the number of data points should be 10 times greater than that of connections in the network.³⁵ The structure of the network can be changed through varying the number of hidden layers as well as the number of neurons in each hidden layer. According to Cybenko, a network that has only one hidden layer is able to approximate almost any type of nonlinear mapping.³⁶ However, the determination of the approximate number of neurons for the hidden layers is difficult and is often done by trial and error. Too few neurons in the hidden layer prevents the network from getting trained appropriately. On the other hand, too many neurons causes the network to respond very well at the training points, but when the network is exposed to new data leads to unacceptably large errors. These problems that occur during neural network training are called "overfitting". Indeed, the network has memorized the training examples, but it has not learned to set up a general correlation between input and output variables. One solution to the overfitting problem is to divide the data points into the training and validation or test data. This method is elaborated in the subsequent sections.

Data Acquisition and Analysis. Perhaps one of the most important decisions in the development of a neuromorphic model is availability of reliable experimental sources of data. The data set used in this work consists of two groups of data: (1) the data set of pure gases, and (2) the data set of binary gas mixtures. The first data group contains the molecular weight, critical temperature, critical pressure, and thermal conductivity at a given temperature. Both hydrocarbons and nonhydrocarbons are among the compounds, and the total number of data points for pure gases is equal to 236.³⁷⁻⁴⁷ The second group of data includes the mixture conductivities at different mole fractions and temperatures. The total number of data points collected for this group is 277.⁴⁸⁻⁶³ Table 1 represents the variety of pure components and binary mixtures used in this study. In Table 2, the thermal conductivity of pure gases is presented at desired temperatures. The ranges of variations of all data applied to the design of ANN models are given in Tables 3 and 4. Much more conductivity data can be found in the references,³⁷⁻⁶³ but

Table 8. Comparison of the Pure Gas MLP with Other Correlations

no.	compound	ref	T	λ_{exp}	λ_{pred}	100 RE ^a ANN	λ	100 RE ^a , other correlations	
			K	W·m ⁻¹ ·K ⁻¹	W·m ⁻¹ ·K ⁻¹		W·m ⁻¹ ·K ⁻¹ , other correlations		
1	Acetone	37	300	0.0115	0.0125	8.69	0.0101 ^c	12.17	
			400	0.0201	0.0211	4.97	0.0187 ^c	6.96	
2	Acetylene	37	293	0.0218	0.0206	5.50	0.0213 ^c	2.29	
			400	0.0332	0.0333	0.30	0.0332 ^c	0.00	
3	Ammonia	37	353	0.0301	0.0292	2.99	0.0355 ^f	17.94	
			400	0.0364	0.0346	4.94	0.0424 ^f	16.48	
4	Argon		273.2	0.0163	0.0173	6.13	0.0166 ^d	1.84	
			491.2	0.0267	0.0280	4.86	0.0265 ^d	0.74	
5	Benzene	46	319.11	0.0126	0.0127	0.79	0.0118 ^c	6.34	
			400	0.0195	0.0199	2.05	0.0189 ^c	3.07	
6	Carbon dioxide	37	273.1	0.0146	0.0148	1.36	0.0147 ^e	0.68	
			39	400	0.0246	0.0249	1.21	0.0248 ^e	0.81
			473	0.0313	0.0305	2.55	0.0306 ^e	2.23	
			39	600	0.0431	0.0398	7.65	0.0402 ^e	6.77
			1100	0.0744	0.0738	0.80	0.0835 ^e	12.23	
7	Carbon monoxide ^b	42	1500	0.0974	0.0980	0.61	^g		
			81.88	0.0071	0.0071	0.00	^g		
			42	91.88	0.0080	0.0079	1.25	^g	
			42	273	0.0221	0.0222	0.45	0.0237 ^c	7.23
			291	0.0237	0.0236	0.42	0.0249 ^e	5.06	
8	Carbon tetrachloride	46	319.11	0.0071	0.0067	5.63	0.0072 ^f	1.40	
			456.88	0.0112	0.0124	10.71	0.0111 ^f	0.89	
9	Chlorine	37	300	0.0089	0.0097	8.98	0.0084 ^e	5.61	
10	Chloroform	46	319.11	0.0080	0.0071	11.25	0.0071 ^c	11.25	
11	Ethane	42	239.11	0.0149	0.0142	4.69	0.0144 ^c	3.35	
			37	300	0.0218	0.0217	0.45	0.0214 ^c	1.83
			37	500	0.0516	0.0496	3.87	0.0509 ^c	1.35
12	Ethyl alcohol ^b	46	293	0.0154	0.0106	31.16	0.0112 ^c	27.27	
			46	373	0.0215	0.0167	22.32	0.0193 ^c	10.23
13	Ethylene ^b	37	250	0.0152	0.0167	9.86	0.0150 ^c	1.31	
			42	273	0.0183	0.0196	7.10	0.0174 ^c	4.91
			37	300	0.0214	0.0230	7.47	0.0203 ^c	5.14
			37	400	0.0342	0.0365	6.72	0.0329 ^c	3.80
			37	500	0.0491	0.0509	3.66	0.0468 ^c	4.68
14	Helium	37	600	0.0653	0.0668	2.29	0.0615 ^c	5.81	
			39	144	0.0928	0.0947	2.04	0.1059 ^d	14.11
			273.2	0.1418	0.1401	1.19	0.1456 ^d	2.67	
			373.2	0.1731	0.1754	1.32	0.1807 ^d	4.39	
			489	0.2250	0.2155	4.22	0.2181 ^d	3.06	
15	Heptane	37	300	0.0120	0.0112	6.66	0.0107 ^c	10.83	
			37	500	0.0325	0.0308	5.23	0.0327 ^c	0.61
16	Hexane ^b	45	273	0.0125	0.0103	17.6	0.0093 ^c	25.6	
			45	298	0.0138	0.0119	13.76	0.0117 ^c	15.21
17	Hydrogen	39	250	0.1561	0.1574	0.83	0.1604 ^e	2.75	
			373	0.2233	0.2166	3.00	0.2156 ^e	3.44	
			39	450	0.2510	0.2513	0.11	0.2418 ^e	3.66
			39	600	0.3150	0.3148	0.06	0.2968 ^e	5.77
			39	800	0.3840	0.3839	0.02	0.3744 ^e	2.50
18	iso-Butane ^b	45	273	0.0138	0.0140	1.44	0.0130 ^c	5.79	
			45	373	0.0241	0.0229	4.97	0.0248 ^c	2.90
19	iso-Pentane ^b	46	273	0.0125	0.0121	3.20	0.0110 ^c	12.00	
			46	373	0.0220	0.0195	11.36	0.0221 ^c	0.45
20	Krypton		491.2	0.0145	0.0153	5.51	0.0149 ^d	2.75	
21	Methane	37	200	0.0218	0.0221	1.37	0.0207 ^c	5.04	
			300	0.0343	0.0361	5.24	0.0322 ^c	6.12	
			400	0.0484	0.0517	6.81	0.0464 ^c	4.13	
22	Methyl acetate ^b	46	273	0.0102	0.0091	10.78	0.0081 ^c	20.58	
			46	293	0.0118	0.0102	13.55	0.0097 ^c	17.79
			46	273	0.0092	0.0111	20.65	0.0088 ^c	4.34
23	Methyl chloride ^b	46	319.11	0.0125	0.0135	8.00	0.0117 ^c	6.40	
			46	373	0.0163	0.0167	2.45	0.0154 ^c	5.52
			46	456.88	0.0225	0.0225	0.00	0.0215 ^c	4.44
			46	484.66	0.0256	0.0247	3.51	0.0236 ^c	7.81
			45	273	0.0135	0.0136	0.74	0.0128 ^c	5.18
24	n-Butane	37	400	0.0264	0.0246	6.81	0.0280 ^c	6.06	
			373.2	0.0580	0.0550	5.17	0.0470 ^d	18.96	
25	Neon		200	0.0186	0.0162	12.90	0.0202 ^e	8.60	
26	Nitric oxide	39	273	0.0230	0.0231	0.43	0.0242 ^c	5.21	
			400	0.0333	0.0325	2.40	0.0326 ^e	2.10	
			900	0.0607	0.0613	0.98	0.0651 ^c	7.24	
27	Nitrogen		273	0.0159	0.0146	8.17	0.0152 ^f	4.40	
28	Nitrous oxide	45, 46	273	0.0128	0.0118	7.81	0.0108 ^c	15.62	
			45, 46	293	0.0144	0.0131	9.02	0.0128 ^c	11.11
29	n-Pentane	45, 46	173	0.0164	0.0164	0.00	0.0189 ^e	15.24	
			39	200	0.0182	0.0185	1.64	0.0195 ^e	7.14
			39	350	0.0307	0.0304	0.97	0.0298 ^e	2.93
			39	500	0.0417	0.0409	1.91	0.0414 ^c	0.71

Table 8 Continued

no.	compound	ref	T	λ_{exp}	λ_{pred}	100 RE ^a ANN	λ	100 RE ^a , other correlations
			K	W·m ⁻¹ ·K ⁻¹	W·m ⁻¹ ·K ⁻¹		W·m ⁻¹ ·K ⁻¹ , other correlations	
31	Propane ^b	37	250	0.0129	0.0131	1.55	0.0121 ^c	6.20
		45	273	0.0151	0.0153	1.32	0.0146 ^c	3.31
		37	300	0.0183	0.0180	1.63	0.0177 ^c	3.27
		45	373	0.0261	0.0258	1.14	0.0271 ^c	3.83
		37	400	0.0295	0.0289	2.03	0.0309 ^c	4.74
		37	500	0.0417	0.0418	0.23	0.0455 ^c	9.11
32	R 12	37	300	0.0097	0.0095	2.06	0.0094 ^f	3.09
		37	373	0.0138	0.0125	9.42	0.0125 ^f	9.42
33	R 21 ^b	37	300	0.0088	0.0082	6.81	0.0082 ^c	6.81
		37	400	0.0135	0.0122	9.62	0.0134 ^c	0.74
		37	500	0.0181	0.0171	5.52	0.0186 ^c	2.76
34	R 22	37	400	0.0170	0.0179	5.29	0.0169 ^c	0.58
35	Sulfur dioxide	41	273	0.0087	0.0087	0.00	0.0096 ^f	10.34
		41	373	0.0119	0.0118	0.84	0.0144 ^f	21.00
36	Water vapor	353	353	0.0218	0.0233	6.88	0.0275 ^f	26.14
		39	450	0.0299	0.0293	2.00	0.0407 ^f	36.12
		39	600	0.0422	0.0424	0.47	0.0573 ^f	35.78
37	Xenon	39	750	0.0549	0.0547	0.36	0.0767 ^f	39.70
		491.2	491.2	0.0093	0.0114	22.58	0.0083 ^d	10.75

^a RE = $|\lambda_{\text{exp}} - \lambda_{\text{pred}}|/(\lambda_{\text{exp}}) \cdot 100$. ^b Not used in the training of the first proposed ANN. ^c The correlation of Misis and Thodos.^{14,15} ^d The correlation of Bromley^{16,17} for pure nonhydrocarbon monatomic gases. ^e The correlation of Bromley^{16,17} for nonhydrocarbon linear molecules. ^f The correlation of Stiel and Thodos.¹⁹ ^g The vapor viscosity is not available for these compounds at given temperature.

all of them are not experimental. In this research, only experimental data points have been utilized.

After identifying and collecting the data set, the next step is the selection of input variables, which are the model's independent variables. The available correlations for prediction of conductivity at constant pressure are essentially based on the assumption that conductivity (λ) can be described as a function of temperature (T), critical temperature (T_c), critical pressure (P_c), and molecular weight (M):

$$\lambda = f(T, T_c, P_c, M) \quad (11)$$

Following this approach, temperature, critical temperature, critical pressure, and molecular weight were used as the inputs of the first ANN model for the prediction of conductivity of pure gases.

The conductivity of gaseous binary mixtures is usually estimated through using semiempirical correlations. These correlations are essentially a function of thermal conductivity, molecular weight, and composition of each component as follows

$$\lambda_{\text{mix}} = f(\lambda_1, \lambda_2, M_1, M_2, x_2) \quad (12)$$

According to eq 12, the inputs of the second ANN model are thermal conductivity of light (λ_2) and heavy (λ_1) component (which can be predicted in the first ANN at the desired temperature), molecular weight of light (M_2) and heavy (M_1) component, and the molar composition of the lighter component (x_2).

Neural Network Training. The multilayer perceptron (MLP) network is used here to develop the predictive models of conductivity for both pure gas and binary gas mixtures. Both proposed MLPs have one hidden layer with a different number of neurons, determined through the constructive approach.⁶⁴ On the basis of the constructive approach, a small number of neurons are used in the hidden layer, and if the error of the trained network does not meet the desired tolerance the number of neurons in the hidden layer is increased one by one. The procedure is continued until the trained network performs satisfactorily (i.e., its training, validation and testing error are lower than the target goals). The Levenberg–Marquardt algorithm was used in the training procedure.^{65–67} Different neural network topologies were compared using their mean relative

errors (MRE) and mean square errors (MSE). The MRE and MSE are defined with the following equations

$$\text{MRE} = \frac{1}{N} \sum_{i=1}^N \frac{|\lambda_{\text{exp}} - \lambda_{\text{pred}}|}{\lambda_{\text{exp}}} \quad (13)$$

$$\text{MSE} = \frac{1}{N} \sum_{i=1}^N (\lambda_{\text{exp}} - \lambda_{\text{pred}})^2 \quad (14)$$

N is the number of data points, and λ_{exp} and λ_{pred} are the experimental and predicted values of thermal conductivity, respectively. Also, the coefficient of determination, R^2 , was used as a measure to evaluate how the trained network estimation is correlated to the experimental data.

The structure of the trained MLP for prediction of pure gas conductivity consists of four neurons in the input layer, ten neurons in the hidden layer, and one neuron at the output layer. The MLP for the estimation of thermal conductivity of a binary mixture of gases has five neurons in the input layer, twelve neurons in the hidden layer, and one neuron at the output layer.

Results and Discussion

Table 5 shows the MRE, MSE, and R values calculated for various neural network configurations, differing with respect to their number of hidden layer neurons. The configuration with minimum error measures (i.e., MRE and MSE) and appropriate R -value was selected as the best network architecture. According to Table 5, the best neural network configuration for prediction of thermal conductivity of pure gases has one hidden layer with ten neurons. Also, an MLP with one hidden layer with twelve neurons is needed for prediction of thermal conductivity of binary gas mixtures. Figure 1 and Figure 2 represent the variation of training errors for the selected MLPs. The parameters (weight and bias values) of the first and the second ANN are shown in Tables 6 and 7, respectively.

Figures 3 and 4 illustrate the correlation between the predictions of the trained MLPs and the corresponding experimental data. The perfect fit is indicated by the solid line. The close proximity of the best linear fit to the perfect fit shows a good correlation among network predictions and experimental data.

Table 9. Comparison of the Second Proposed MLP with Other Correlations

no.	gas mixture	ref	T/K	x_2	$\lambda_{\text{mix,exp}}$	$\lambda_{\text{mix,pred}}$	100 RE ANN	λ_{mix}	100 RE, other correlations
					$\text{W}\cdot\text{m}^{-1}\cdot\text{K}^{-1}$	$\text{W}\cdot\text{m}^{-1}\cdot\text{K}^{-1}$		$\text{W}\cdot\text{m}^{-1}\cdot\text{K}^{-1}$, other correlations	
1	$\text{H}_2 + \text{N}_2$	56	273.16	0.795	0.1053	0.1113	5.65	0.1109 ^b	5.35
				61	366.16	0.408	0.0766	0.0760	0.78
				0.662	0.1161	0.1159	0.20	0.1197 ^c	3.1
				0.853	0.1590	0.1622	2.02	0.1623 ^c	2.1
2	$\text{H}_2 + \text{O}_2$	57	295	0.5	0.0763	0.0753	1.36	0.0700 ^b	8.3
		61	338.16	0.509	0.0868	0.0872	0.45	0.0898 ^c	3.4
3	$\text{H}_2 + \text{Ar}^d$	56	273.16	0.09	0.0229	0.0224	2.34	0.0212 ^b	7.45
				0.18	0.0305	0.0293	3.91	0.0270 ^b	11.35
		0.40	0.0526	0.0496	5.78	0.0454 ^b	13.7		
		0.60	0.0781	0.0745	4.58	0.0700 ^b	10.35		
4	$\text{N}_2 + \text{Ar}$	58	273.16	0.3587	0.0186	0.0176	5.38	0.0198 ^b	7.2
		5	He + Ar	40	273.16	0.847	0.0969	0.0975	0.61
6	$\text{H}_2 + \text{D}_2$	40	273.16	0.496	0.1465	0.1480	1.03	0.1507 ^d	2.9
				60	338.16	0.503	0.1593	0.1604	0.69
		60	368.16	0.064	0.1940	0.1877	3.26	0.1905 ^c	1.8
				0.238	0.1731	0.1739	0.46	0.1688 ^c	2.5
7	$\text{H}_2 + \text{CO}_2$	40	273.16	0.512	0.1597	0.1557	2.50	0.1639 ^c	2.6
				0.757	0.1593	0.1505	5.54	0.1599 ^c	0.4
		448.16	0.238	0.1797	0.1813	0.87	0.1759 ^c	2.1	
		0.170	0.0253	0.0253	0.00	0.0247 ^d	2.6		
8	He + O ₂	40	298.16	0.370	0.0432	0.0431	0.21	0.0411 ^d	4.9
				0.607	0.0720	0.0730	1.37	0.0697 ^d	3.2
		59	303.16	0.834	0.1169	0.1156	1.09	0.1140 ^d	2.5
				0.906	0.1463	0.1465	0.13	0.1468 ^d	0.4
9	Ne + O ₂	59	303.16	0.10	0.0319	0.0301	5.49	0.0317 ^e	0.62
				0.25	0.0403	0.0400	0.66	0.0401 ^e	0.49
		0.40	0.0514	0.0516	0.43	0.0509 ^e	0.97		
		0.55	0.0654	0.0653	0.14	0.0661 ^e	1.07		
10	O ₂ + Kr	59	303.16	0.70	0.0842	0.0839	0.32	0.0856 ^e	1.66
				0.85	0.1129	0.1106	2.02	0.1120 ^e	0.79
		318.16	0.10	0.0330	0.0321	2.64	0.0323 ^c	2.12	
		0.1461	0.0354	0.0352	0.64	0.0366 ^c	0.67		
11	O ₂ + Xe	59	303.16	0.8364	0.1145	0.1120	2.14	0.1153 ^c	0.69
				0.85	0.1169	0.1148	1.76	0.1167 ^e	0.17
		0.1398	0.0296	0.0299	0.91	0.0298 ^c	0.67		
		0.2366	0.0311	0.0308	0.95	0.0320 ^c	2.89		
12	Ar + SO ₂	63	312.16	0.4096	0.0340	0.0332	2.36	0.0358 ^c	5.29
				0.5764	0.0374	0.0366	2.02	0.0395 ^c	5.61
		63	394.46	0.392	0.0174	0.0166	4.87	0.0171 ^e	3.01
		63	434.26	0.619	0.0208	0.0203	2.57	0.0209 ^e	1.45
12	Ar + SO ₂	63	473.76	0.7749	0.0426	0.0420	1.31	0.0436 ^c	2.34
				0.504	0.0375	0.0358	4.41	0.0352 ^c	6.2
		0.1152	0.0308	0.0310	0.51	0.0305 ^c	0.97		
		0.2993	0.0325	0.0328	1.01	0.0347 ^c	6.76		
12	Ar + SO ₂	63	353.26	0.4844	0.0353	0.0359	1.61	0.0389 ^c	10.1
				0.6515	0.0389	0.0399	2.49	0.0425 ^c	9.25
		0.7420	0.0421	0.0424	0.79	0.0444 ^c	5.46		
		0.8403	0.0451	0.0452	0.21	0.0462 ^c	2.43		
12	Ar + SO ₂	63	394.46	0.261	0.0451	0.0441	2.10	0.0435 ^c	3.6
				0.504	0.0422	0.0402	4.68	0.0395 ^c	6.3
		63	434.26	0.619	0.0208	0.0203	2.57	0.0209 ^e	1.45
		63	473.76	0.442	0.0218	0.0211	3.25	0.0219 ^e	3.79

Table 9 Continued

no.	gas mixture	ref	T/K	x_2	$\lambda_{\text{mix,exp}}$	$\lambda_{\text{mix,pred}}$	100 RE ANN	λ_{mix}	100 RE, other correlations
					$\text{W}\cdot\text{m}^{-1}\cdot\text{K}^{-1}$	$\text{W}\cdot\text{m}^{-1}\cdot\text{K}^{-1}$		$\text{W}\cdot\text{m}^{-1}\cdot\text{K}^{-1}$, other correlations	
13	SO ₂ + Kr	63	312.16	0.432	0.0101	0.0089	12.02	0.0100 ^c	0.99
			353.26	0.592	0.0121	0.0123	1.57	0.0118 ^e	2.47
			394.46	0.404	0.0139	0.0139	0.00	0.0132 ^e	5.03
			434.26	0.598	0.0162	0.0162	0.00	0.0155 ^e	4.32
			473.76	0.436	0.0171	0.0168	2.01	0.0165 ^e	3.50
14	He + Kr ^a	62	302.16	0.240	0.0226	0.0261	15.40	0.0228 ^b	0.88
				0.422	0.0371	0.0399	7.52	0.0371 ^b	0.00
				0.490	0.0431	0.0456	5.78	0.0437 ^b	1.39
				0.577	0.0535	0.0538	0.47	0.0537 ^b	0.37
				0.750	0.0807	0.0794	1.62	0.0806 ^b	0.12
		0.880	0.1091	0.1075	1.47	0.1109 ^b	1.64		
15	Kr + Xe	62	302.16	0.158	0.0062	0.0061	1.05	0.0062 ^b	0.00
16	H ₂ + Ne	60	366.16	0.595	0.1321	0.1288	2.50	0.1388 ^c	5.1
			368.16	0.728	0.1509	0.1519	0.69	0.1652 ^c	9.5
17	Ne + N ₂	60	366.16	0.195	0.0342	0.0341	0.38	0.0337 ^c	1.5
			368.16	0.744	0.0422	0.0460	8.89	0.0510 ^c	20.9
18	N ₂ + O ₂	61	313.16	0.238	0.0272	0.0276	1.50	0.0272 ^c	0.0
			366.16	0.751	0.0313	0.0313	0.00	0.0305 ^c	2.4
			408.16	0.486	0.0355	0.0351	1.12	0.0328 ^c	7.7
19	H ₂ + Kr	60	338.16	0.531	0.0698	0.0707	1.22	0.0723 ^c	3.6
20	H ₂ + Xe	60	313.16	0.566	0.0648	0.0632	2.54	0.0625 ^c	3.5
21	D ₂ + Xe	60	366.16	0.504	0.0493	0.0482	2.21	0.0455 ^c	7.7
22	D ₂ + N ₂	61	338.16	0.399	0.0578	0.0583	0.88	0.0588 ^c	1.7
				0.778	0.1004	0.1009	0.46	0.1033 ^c	2.9

^a Not used in the training of the second proposed ANN. ^b The correlation of Wassiljewa.⁴⁹ ^c The correlation of Mason and Saxena.²¹ ^d The correlation of Lindsay and Bromley.²² ^e The correlation of Hirschfelder.²⁶

A test data set, consisting of 96 data points, was used to verify the capability of the developed MLP in prediction of pure gas conductivity. In the same way, the designed MLP model for mixture conductivity was tested through applying a set of data with 99 data points covering 22 different pairs of components. It should be noted that none of the test data were used in the training of both networks. Applying aforementioned test data sets on the pure gas MLP and the mixture gas MLP indicates both networks are generalizable with a good accuracy: for the pure gas MLP, the values of MRE and MSE are 5.4 % and $3.8\cdot 10^{-6}$; for the mixture gas MLP, the values of MRE and MSE are 2.2 % and $3.3\cdot 10^{-6}$, respectively.

Figure 5 indicates the correlation between predicted and experimental values of pure gas conductivities for the test data set. Such a correlation is also illustrated in Figure 6 for binary gaseous mixtures. The correlation coefficients of the data shown in Figures 5 and 6 are 0.9996 and 0.9993, respectively. These *R* values represent a very good correlation between the simulated and the experimental test data.

Table 8 summarizes the results of applying the developed MLP model and other methods to predict the thermal conductivity of pure gases. Making a comparison among the predictions of the MLP and other proposed methods to the experimental data shows that the accuracy of the developed MLP is much better than that of other methods. Furthermore, the number of input variables needed by the MLP to predict the pure gas conductivity is less than most of the other alternative methods. While no unique correlation exists to estimate the conductivity for all components over a broad range of temperatures in Table 8, the developed MLP model can do that very well. In each case, the appropriate correlation was selected based on the recommendations given in the literature. For instance, Bromley^{16,17} suggested two distinct correlations to predict the gas thermal conductivity of pure nonhydrocarbon monatomic gases and nonhydrocarbon linear molecules at low pressure (up to 1 bar). Also, Stiel and Thodos¹⁹ proposed a correlation for pure nonhydrocarbon nonlinear molecules at low pressure (up to 1 bar). These correlations have higher average errors for polar

compounds (e.g., ammonia, sulfur dioxide, and water vapor in Table 8). Stiel and Thodos's equations require (in addition to temperature, critical temperature, critical pressure, and molecular weight) accurate values for the heat capacity at constant volume and also vapor viscosity which is usually not available for all compounds at any temperature. Misis and Thodos^{14,15} developed two correlations for low-pressure (< 350 kPa) hydrocarbon gases. One of their correlations was proposed for methane and cyclic compounds below reduced temperatures of 1.0, and the other one was recommended for all hydrocarbons above reduced temperatures of 1.0. These correlations, in addition to the input data needed for the neural network model, require the heat capacity at constant pressure. The pure gas MLP proposed in this article is based on the critical temperature, critical pressure, and molecular weight that is available for all gases.

Experimental data for conductivities of binary systems at different temperatures and compositions are presented in Table 9. For each data point in this table, the mixture conductivity was calculated by the proposed MLP, and the value estimated by existing correlations was obtained from the literature. Four types of formulas used in this table were selected from the works of Wassiljewa,⁴⁹ Mason and Saxena,²¹ Lindsay and Bromley,²² and Hirschfelder.²⁶ Wassiljewa's correlation, which is based on the kinetic theory of gases, underestimates significantly the thermal conductivities of gaseous mixtures.⁴⁹ The formula of Hirschfelder was used to estimate conductivities (λ_{mix}) of O₂ + He, O₂ + Kr, and O₂ + Xe mixtures.²⁶ The thermal conductivity of the pure component needed in Hirschfelder's formula was obtained from experimental data. The accuracy of the Hirschfelder's method is very good and comparable to that of the designed MLP in this work. In the case of SO₂ + Kr, the force parameters needed in Hirschfelder's correlation ($\epsilon_{12}/k = 244$ K; $\sigma_{12} = 3.808$ Å) were determined from diffusion data,⁶⁸ but because of unavailability of reliable diffusion data for the SO₂ + Ar system, the force parameters ($\epsilon_{12}/k = 280$ K; $\sigma_{12} = 3.392$ Å) were determined from binary viscosity data.⁶⁹ For 47 experimental data points, the procedure of Mason and Saxena²¹ leads to an average relative error of 4.4 % while the proposed

MLP has an average relative error of 1.8 %. Also, comparing the results of the Lindsay and Bromley correlation to that of the MLP method shows that the relative error of the MLP is much better. For instance, the average relative error of the Lindsay and Bromley method for $\text{H}_2 + \text{CO}_2$ is 2.7 %, while for the proposed neural network it is 0.56 %.

Comparing the relative errors of the methods in Table 9 reveals that the overall accuracy of the designed MLP is more than that of other suggested correlations. Furthermore, the number of input variables required for the proposed MLP model is less than that of most other alternative methods. The developed mixture gas MLP predicts the mixture conductivity based on the pure component conductivity (which can be estimated from the pure gas MLP at desired temperatures), molecular weight of pure component, and composition of the light component. While some of the binary mixtures of gases shown in the table were not used in the training of the MLP model, we applied intentionally them to the network to assess its extrapolation capability. It should be notified that prediction of thermal conductivity of the binary mixture of gases by other proposed correlations is really tedious and boring, while the developed network scheme is easy to use and requires fewer input properties which are usually available for most gases.

Conclusions

In this research, an artificial network scheme was developed to approximate the thermal conductivities of binary gaseous mixtures. The proposed scheme consists of two consecutive multilayer perceptrons (MLPs). Critical temperature, critical pressure, molecular weight, and the gas temperature are fed to the first MLP by which the pure gas conductivity is approximated for use in the next MLP. The second MLP estimates the binary mixture conductivity from the conductivities and molecular weights of both components as well as the mole fraction of the lighter component. Both networks were trained and verified by using a large experimental data set of pure and mixture gas conductivities over wide ranges of temperatures and molecular structures. Also, we applied four different correlations, recommended in the literature, to the experimental data points. Comparing the errors of the developed network scheme and other suggested correlations reveals that the neural network model can predict the thermal conductivities of the pure and binary gaseous mixture remarkably better than other suggested methods. Some advantages can be mentioned for the neural network model over other alternative correlations: (1) compressing a vast range of experimental thermal conductivities of pure and mixed gases in an easy to use and accurate neural model, (2) predicting pure gas conductivity through a single MLP model over wide ranges of temperatures and molecular structures, rather than using alternative correlations validated across limited ranges of temperatures and substances, (3) requiring fewer physical input parameters which are commonly available for all components.

The results of applying the trained MLP model to the test data indicate that this method has very good interpolation and extrapolation capabilities with respect to not only change in temperature range but also molecular structure.

Literature Cited

- Chapman, S.; Cowling, T. G. *The Mathematical Theory of Non-Uniform Gases*; Cambridge University Press: London, 1953.
- Hirschfelder, J. O.; Bird, R. B. *The Molecular Theory of Gases and Liquids*; Wiley: New York, 1954.
- Ubbelohde, A. R. The Thermal Conductivity of Polyatomic Gases. *J. Chem. Phys.* **1935**, *3*, 219.
- Tye, R. P. *Thermal Conductivity*; Academic Press: London and New York, 1969; Vol. 2.
- Longuet-Higgins, H. C.; Pople, J. A. Transport Properties of a Dense Fluid of Hard Spheres. *J. Chem. Phys.* **1956**, *25*, 884.
- Horrocks, J. K.; McLaughlin, E. Non-Steady-State Measurements of the Thermal Conductivities of Liquid Polyphenyls. *Proc. R. Soc.* **1963**, *273*, 259.
- Horrocks, J. K.; McLaughlin, E. Temperature Dependence of the Thermal Conductivity of Liquids. *Trans. Faraday Soc.* **1963**, *59*, 1709.
- Longuet-Higgins, H. C.; Valleau, J. P. Transport coefficients of dense fluids of molecules interacting according to a square well potential. *Mol. Phys.* **1958**, *1*, 284.
- Davis, H. T.; Rice, S. A.; Sengers, J. V. On the Kinetic Theory of Dense Fluids. IX. The Fluid of Rigid Spheres with a Square-Well Attraction. *J. Chem. Phys.* **1961**, *35*, 2210–2233.
- Sengers, J. V. Divergence in the Density Expansion of the Transport Coefficients of a Two-Dimensional Gas. *Phys. Fluids* **1966**, *9*, 1685–1696.
- Choh, S. T.; Uhlenbeck, G. E. *The Kinetic Theory of Phenomena in Dense Gases*; University of Michigan Report: 1958.
- Cohen, E. G. D. *Statistical Mechanics of Equilibrium and Non-equilibrium Processes*; Meixner, J., Ed.; North-Holland: Amsterdam, 1965.
- Bogolubov, G. N. N. *Studies in statistical Mechanics*; de Boer, J., Uhlenbeck, G. E., Eds.; North-Holland, Amsterdam, 1962; Vol. 7.
- Misic, D.; Thodos, G. Thermal Conductivity of Hydrocarbon Gases at Normal Pressures. *AIChE J.* **1961**, *7*, 264.
- Misic, D.; Thodos, G. Atmospheric Thermal Conductivity for Gases of Simple Molecular Structure. *J. Chem. Eng. Data* **1963**, *9*, 540.
- Bromley, L. A. *Thermal Conductivity of Gases at Moderate Pressures*; University of California Radiation Laboratory, Report No. UCRL-1852, Berkeley, CA 1952.
- Bromley, L. A.; Wilke, C. R. Viscosity Behavior of Gases. *Ind. Eng. Chem.* **1951**, *43*, 1641–1648.
- Pliński Edward, F.; Witkowski Jerzy, S. Prediction of the thermal properties of CO_2 , CO, and Xe laser media. *Opt. Laser Technol.* **2001**, *32*, 61–66.
- Stiel, L. I.; Thodos, G. The thermal conductivity of nonpolar substances in the dense gaseous and liquid regions. *AIChE J.* **1964**, *10*, 26–32.
- Muckenfuss, C.; Curtiss, C. F. Thermal Conductivity of Multicomponent Gas Mixtures. *J. Chem. Phys.* **1958**, *29*, 1273.
- Mason, E. A.; Saxena, S. C. Thermal Conductivity of Multicomponent Gas Mixtures. II. *J. Chem. Phys.* **1959**, *31*, 511–518.
- Lindsay, A. L.; Bromley, L. A. Thermal Conductivity of Gas Mixtures. *Ind. Eng. Chem.* **1950**, *43*, 1508–1511.
- Srivastava, B. N.; Saxena, S. C. Thermal Conductivity of Binary and Ternary Rare Gas Mixtures. *Proc. Phys. Soc. (London)* **1957**, *B70*, 583.
- Saxena, S. C. Thermal Conductivity of Binary and Ternary Mixtures of Helium, Argon and Xenon. *Indian J. Phys.* **1957**, *31*, 597–606.
- Ulybin, S. A.; Bugrov, V. P.; Vulyin, A. V. Temperature Dependence of Thermal Conductivity of Nonreacting Low Density Gas Mixtures. *Teplofizika Vysokikh Temperatur* **1966**, *4*, 210.
- Hirschfelder, J. O. *Sixth International Combustion Symposium*; P 351, Reinhold: New York, N. Y., 1957.
- Ignacio, J.; Turias, J.; Gutiérrez, M.; Galindo, P. L. Modeling the effective thermal conductivity of a unidirectional composite by the use of artificial neural networks. *Compos. Sci. Technol.* **2005**, *65*, 609–619.
- Sablani, S. S.; Shafiq, R. M. Using neural networks to predict thermal conductivity of food as a function of moisture content, temperature, and apparent porosity. *Food Res. Int.* **2003**, *36*, 617–623.
- Sablani, S. S.; Oon-Doo, B.; Marcotte, M. Neural networks for predicting thermal conductivity of bakery products. *J. Food Eng.* **2002**, *52*, 299–304.
- Therdthai, N.; Weibiao, Z. Artificial neural network modeling of the electrical conductivity property of recombined milk. *J. Food Eng.* **2001**, *50*, 107–111.
- Jalali-Heravi, M.; Fatemi, M. H. Prediction of thermal conductivity detection response factor using an artificial neural networks. *J. Chromatogr.* **2000**, *897*, 227–235.
- Eslamloueyan R.; Khademi M. H. Estimation of Thermal Conductivity of Pure Gases by Using Artificial Neural Networks. *Int. J. Thermal Sci.* **2008**, in press.
- Hagan, M. T.; Demuth, H. B.; Beale, M. H. *Neural Network Design*; PWS Publishing: Boston, MA, 1996.
- Boozarjomehri, R.; Abdolahi, F.; Moosavian, M. A. Characterization of basic properties for pure substances and petroleum fractions by neural network. *Fluid Phase Equilib.* **2005**, *231*, 188–196.
- Statistical Neural Networks, User's Manual, Release 4.0 F*, Statsoft: Tulsa, OK, 2000.
- Cybenko, G. V. Mathematics of control. *Signals Syst.* **1989**, *2*, 303–314.

- (37) Perry, R. H.; Green, D. W. *Perry's chemical engineers handbook*, 7th ed.; McGraw Hill: New York, 1997.
- (38) Reid, R. C.; Prausnitz, J. M.; Poling, B. E. *The Properties of Gases and Liquids*, 4th ed., McGraw-Hill: New York, 1987.
- (39) Holman J. P. *Heat Transfer*, 8th ed.; McGraw-Hill: United States of America, 1997.
- (40) Tseederberg, N. V. *Thermal Conductivity of Gases and Liquids*; Robert, D., Ed.; M.I.T. Press: Cambridge, Mass, 1965.
- (41) Dickens, B. G. The Effect of Accommodation on Heat Conduction Through Gases. *Proc. R. Soc. A (London)* **1934**, 850, 517.
- (42) Eucken, A. On the temperature dependence of the thermal conductivity of some gases (in German). *Physik. Z.* **1911**, 12, 1101–1107.
- (43) Gregory, H.; Marshall, S. Thermal Conductivities of Oxygen and Nitrogen. *Proc. R. Soc. A (London)* **1928**, 118, 594–607.
- (44) Washburn, E. W., Ed. *International Critical Tables*; McGraw-Hill: New York, 1929.
- (45) Mann, W. B.; Dickens, B. G. The Thermal Conductivities of the Saturated Hydrocarbons in the Gaseous. *Proc. R. Soc. A (London)* **1931**, (823), 77.
- (46) Moser, E. Dissertation, Berlin, 1913.
- (47) Sherratt, G. G.; Griffiths, E. A hot-wire method for the thermal conductivity of gases. *Phil. Mag.* **1939**, 27, 68.
- (48) Carmichael, L. T.; Jackobs, J.; Sage, B. H. Thermal Conductivity of fluids, A mixture of methane and n-Butane. *J. Chem. Eng. Data* **1968**, 3 (4), 489.
- (49) Wassiljewa, A. Heat-Conduction in gaseous mixtures. *Phys. Z.* **1904**, 5 (22), 737–742.
- (50) Grüss, H.; Schmick, H. *Siemens Konzern* **1928**, VII (1), 202.
- (51) Ibbs, T. L.; Hirst, A. A. The Thermal Conductivity of Gas Mixtures. *Proc. R. Soc. Ser. A* **1929**, 123 (791), 134–142.
- (52) Waschmuth, J. *Phys. Z., Leipzig* **1908**, No. 7 (The original data of Waschmuth is reproduced in ref 40).
- (53) Kornfield, G.; Hilferding, K. *Z. Phys. Chem., Ergänzungsband Bodenstein Festband*, **1931**, 792 (The original data of Kornfield and Hilferding is reproduced in ref 40).
- (54) Weber, S. Theoretical and Experimental Study of Thermal Conductivity of Gas Mixtures. *Ann. Phys.* **1917**, 359 (23), 481.
- (55) Archer, C. T. Thermal Conduction in Hydrogen-Deuterium Mixtures. *Proc. R. Soc. Ser. A* **1938**, 165, 474.
- (56) Kihara, T. Determination of Intermolecular Forces from the Equation of State of Gases. II. *J. Phys. Soc. Jpn.* **1951**, 6 (3), 184.
- (57) Bird, R. B. Dissertation, University of Wisconsin, 1950.
- (58) Bird, R. B.; Spatz, E. L.; Hirschfelder, J. O. The Third Virial Coefficient for Non-Polar Gases. *J. Chem. Phys.* **1950**, 18, 1359.
- (59) Srivastava, B. N.; Barua, A. K. Thermal Conductivity of Binary Mixtures of Diatomic and Monatomic Gases. *J. Chem. Phys.* **1960**, 32 (2), 427–435.
- (60) Saxena, S. C.; Tondon, P. K. Experimental Data and Procedures for Predicting Thermal Conductivity of Binary Mixtures of Nonpolar Gases. *J. Chem. Eng. Data* **1971**, 16 (2), 212–220.
- (61) Saxena, S. C.; Gupta, G. P. Experimental Data and Procedures for Predicting Thermal Conductivity of Multicomponent Mixtures of Nonpolar Gases. *J. Chem. Eng. Data* **1970**, 15 (1), 98–107.
- (62) Brokaw, R. S. *Approximate Formulas for Viscosity and Thermal Conductivity of Gas Mixtures*; Lewis Research Center Cleveland: OH, 1964.
- (63) Das Gupta, A. Thermal Conductivity of Binary Mixtures of Sulphur Dioxide and Inert Gases. *Int. J. Heat Mass Transfer* **1967**, 10, 921–929.
- (64) Haykin S. *Neural Networks: A Comprehensive Foundation*, 2nd ed.; Prentice-Hall: Englewood Cliffs, NJ, 1999.
- (65) Levenberg, K. A method for the solution of certain problems in least squares. *SIAM J. Numer. Anal.* **1944**, 16, 588–604.
- (66) Marquardt, D. An algorithm for least-squares estimation of nonlinear parameters. *SIAM J. Appl. Math.* **1963**, 11, 431–441.
- (67) Hagan, M. T.; Menhaj, M. Training Feedforward Networks with the Marquardt Algorithm. *IEEE Trans. Neural Netw.* **1994**, 5, 989–993.
- (68) Srivastava, B. N.; Saran, A. Mutual diffusion in polar-nonpolar gases: krypton-sulphur dioxide and krypton-diethyl ether. *Can. J. Phys. (Paris)* **1966**, 44, 2595.
- (69) Chakraborti, P. K.; Gray, P. Viscosities of gaseous mixtures containing polar gases; mixtures with one polar constituent. *Trans. Faraday Soc.* **1965**, 61, 2422.

Received for review September 22, 2008. Accepted November 15, 2008.

JE800706E